University of Nairobi

School of Engineering

DEPARTMENT OF GEOSPATIAL AND SPACE TECHNOLOGY

The Use of Google Earth Engine to Analyse Changes in Vegetation Cover within Shompole and Olkirimatian Group Ranches, Kenya

BY

Stephen Oloo

F56/7250/2017

A project submitted in partial fulfilment of the requirements for the Degree of Master of Science in Geographic Information Systems, in the Department of Geospatial and Space Technology of the University of Nairobi

August 2020

Declaration of originality

Name of student:	Stephen Owambo Oloo
Registration:	F56/7250/2019
College:	Architecture and Engineering
Faculty/School/Institute:	Engineering
Department:	Geospatial and Space Technology
Course Name:	Msc. Geographic Information System
Title of work:	The Use of Google Earth Engine to Analyse Changes in Vegetation Cover within Shompole and Olkirimatian Group Ranches, Kenya

1) I understand what plagiarism is and I'm aware of the university policy in this regard
2) I declare that this research project is my original work and has not been submitted elsewhere for examination, award of a degree or publication. Where other works or my own work has been used, this has properly been acknowledged and referenced in accordance with the University of Nairobi's requirements
3) I have not sought or used the services of any professional agencies to produce this work
4) I have not allowed, and shall not allow anyone to copy my work with the intention of passing it off as his/her work
5) I understand that any false claim in respect of this work shall result in disciplinary action in accordance with University of Nairobi anti-plagiarism policy

Signature:

Date:

Turn it in report summary

STUDENT:

MR. STEPHEN OWAMBO OLOOO: SIGNATURE……..DATE……..……..

SUPERVISORS:

MR. OKUMU BENSON M.: SIGNATURE……..DATE……..……..

xxxxxxxxxxxxxxx: SIGNATURE……..DATE……..

Acknowledgement

I could not have done this on my own, I received support from various individuals one of them being my supervisor Mr Benson Okumu whom I am much indebted to for the guidance he offered me at every step of this project. I wish to acknowledge my parents Mr. George Oloo and Mrs Phelesia Akinyi for the moral support they offered me during this project it wouldn't have been possible without their wise advice. I also wish to thank the department of Geospatial Engineering for offering the opportunity to learn the skills that have made the completion of this project possible. To finish, I wish to give glory to God for enabling me to reach this far.

Table of contents

List of Figures

List of Tables

List of Equations

Abstract

Livestock production contribute to nearly a half of agricultural GDP in the country and is the main source of livelihood for the pastoral nomadic communities. These pastoral communities depend on rangelands to provide water and forage to their livestock. In the recent past, there have been unprecedented changes in land cover across Kenya's rangelands. This have resulted into diminishing grazing areas for the pastoral communities. This study exploits Google Earth Engine (GEE) capabilities to analyse land use land cover changes in Shompole and Olkirimatian group ranches by looking into the changes in total vegetation fractional canopy (TVFC) cover . The study finds that there has been a continuous increase in TVFC cover within the group ranches with major increase coinciding with the intervention work being implemented by the South Rift Association of Land Owners (SORALO). Secondly, it shows that TVFC cover remain higher in farming areas. And last but not least, it highlights the shifting phenomenon of the Shompole swamp. These finding demonstrate, GEE capabilities as a tool that can be utilised in rangeland management.

CHAPTER 1: INTRODUCTION

1.1 Background

Livestock production contributes to nearly half of Kenya's agricultural GDP. A huge chunk contributing to this economic benefit comes from ruminant production. Farmers also draw a wide range of benefits from livestock that include; source of income for the pastoralists; draught animals for crop farmers; and to others, livestock are viewed as insurance that can be liquidated during emergencies(ICPALD, 2013; Ouma, Obare, & Staal, 2003).

Ruminant production in the country largely depends on natural rangelands which are highly influenced by the variability of rainfall, the efficiency by which rainfall is converted into usable forage, the use of the grazing resources by domestic and wild herbivores, and the relationship between quantity and quality of the range resources(Bekure, de Leeuw, Grandin, & Neate, 1991). Recent studies have shown that continuous grazing and overgrazing in the rangelands leads to loss of vegetation with negative, long-term effects on grass functional qualities and forage production(Angassa, 2014; KIOKO et al., 2012; Mganga, Musimba, & Nyariki, 2015). Together with unplanned land subdivision and developments, changing land tenure systems, crop farming, sedentarisation poses a great threat to these rangelands(Muriithi, 2016; Waithaka, 2004). It is, therefore, necessary to ensure proper management of these rangelands and to livestock production as a whole.

The government together with non-governmental institutions have been on the forefront in the formation and sensitisation of pastoralist communities, who own the largest share of livestock in the country, on the importance of rangeland management. Several group ranches have therefore been established across the country in regions dominated by pastoralist to enable the management of rangelands and hence improve livestock productivity(Measham & Lumbasi, 2013; Mureithi & Opiyo, 2010). Managerial techniques employed in these group ranches are mostly based on controlling access to the grazing areas and non can be used to assess the nature of vegetation, the quantity of grassland and encroached areas in time and also support sustainable planning of the rangelands(Measham & Lumbasi, 2013; Mganga et al., 2015; Mureithi & Opiyo, 2010). Remote sensing can play a key role in filling this gap.

The history of the application of remote sensing technology in rangelands management dates back to the 80s(Tueller, 1989). Remote sensing technology is a useful tool for rangeland management as it enables the estimation of biodiversity at a landscape scale and in detecting and tracking of land cover land-use changes, land degradation, and fire within the rangelands(Reeves et al., 2016). Despite the huge benefits that come with remote sensing, there are also some challenges. Some of the challenges include; huge volumes of remote sensing data, data with different projections, data with different spatial, spectral and resolution, and data in different formats(Ma et al., 2015). These puts so much strain on the traditional remote sensing technologies.

One of the recent technologies that have shown potential to mitigate these challenges is cloud computing. Several tools have been developed for cloud computing in the geospatial industry that includes Hadoop, GeoSpark, TerraLib, GeoMesa, and Google Earth Engine (GEE)(Ma et al., 2015). Google Earth Engine is a cloud-based platform that makes it easy to access high-performance computing resources for processing very large geospatial datasets(Gorelick et al., 2017), without having to worry about computing requirements. In this study, we are going to investigate the effectiveness of using GEE analysing and mapping land use land cover changes in pastoral rangeland in Kenya

1.2 Problem Statement

Livestock production is a way of life and the main source of income to pastoral communities who form 10% of the total population and 13% of the rural population in Kenya(Krätli & Swift, 2014). All the pastoral communities depend on rangelands to feed their livestock. These rangelands are susceptible to continuous and abrupt anthropogenic changes and climate change effects that might cause huge loses to these pastoral communities hence the need to incorporate detailed timely remote sensing analysis in rangeland management.

The rampant increase in population across pastoralist regions which is driving unplanned / poorly planned development, rapid sedentarisation, alienation of pastoral land, and conversion of wet-season pasture land to other land uses has greatly led to shrinking of rangeland areas(Humanitarian Policy Group, 2010). This has led to continuous grazing and overgrazing within the limited rangeland resources. The impact of these activities has not been investigated and mapped within

the Kenyan rangelands. It is, therefore, wiser to use remote sensing technology in rangeland management to quantify this impact.

Improvement in remote sensing technologies have introduced new challenges such as an increase in data volume and increase in data complexity. This has made traditional remote sensing technologies (i.e. obtaining satellite data and analysing it on a personal computer) almost impossible and extremely expensive. As this creates a huge demand for computer hardware capabilities and remote sensing software capabilities which in turn drives up the cost of carrying out remote sensing analysis(Ma et al., 2015). It is therefore important to investigate on a cheaper and faster alternative.

1.3 Objectives

This study aims to detect, analyse and map changes in vegetation cover within Shompole and Olkirimatian group ranches in Kenya using GEE.

1.4 Specific Objectives

i. Use GEE to determine the fractional canopy cover.
ii. Assess the temporal trend of the fractional canopy cover using GEE.
iii. Use GEE to compute areas that define areas with significant changes in vegetation cover spatially.

1.5 Justification for the Study

Land cover is changing every day in the study area due to varying pastoral sedentarization levels, social-economic development, overgrazing, and conservation initiatives. This study will inform the community about the impact of these changes.

Evidence from recent studies has raised concern on the decreasing extent of the African savannah grasslands. This study aims to point out where this occurs in the southern rangelands of Kenya and assist rangeland managers to allocate conservation resources appropriately.

1.6 Scope of work

This project aims to explore the potential of dense time-series data available within the GEE platform to detect changes on rangelands in Kenya. The study site will focus on Olkirimatian and Shompole group ranches located in Kajiado. The project will focus on monitoring both green and senescent vegetation cover. In doing so, this project will also assess the impact of a community organisation working within the study area to improve rangeland conditions and increase biodiversity. The work in this project will include, data collection, analysis, and presentation.

CHAPTER 2: LITERATURE REVIEW

2.1 Livestock Production in Kenya

Livestock production contributes to nearly half of Kenya's agricultural GDP. A huge chunk of this economic benefit comes from ruminant production. Farmers also draw a wide range of benefits from livestock that include; source of income for the pastoralists; draught animals for crop farmers; and to others, livestock are viewed insurance that can be liquidated during emergencies(ICPALD, 2013; Ouma et al., 2003).

A huge proportion of ruminant production is carried out by pastoral communities who live in the arid and semiarid fringes of the country. They move their livestock from place to place to minimise drought losses. However, recently there has been a growing concern over access to dry season grazing pasture and water in the arid and drought prone areas inhabited by these communities. This has led to low livestock production(Mureithi & Opiyo, 2010).

As most of the pastoralist depend on rangelands for forage for their livestock, this dependence raises numerous concerns about the health, maintenance, and management of rangelands from local to global perspectives.

2.2 Rangeland management systems in Kenya

According to the Society for Range Management, rangelands can be defined as the land on which the indigenous vegetation (climax or natural potential) is predominantly grasses, grass-like plants, forbs, or shrubs and is managed as a natural ecosystem. If plants are introduced, they are managed similarly. Rangelands include natural grasslands, savannas, shrublands, many deserts, tundra, alpine communities, marshes, and wet meadows(SRM, 2019).

Management of rangelands in Kenya is done through group ranches. A group ranch is a livestock production system or enterprise where a group of people jointly own freehold title to land, maintain agreed stocking levels and herd their livestock collectively which they own individually. The selection of members to a particular group ranch is based on kinship and traditional land rights. The objectives of group ranches are to increase the productivity of pastoral lands through increased

off-take, to improve the earning capacity of pastoralists, to avoid possible landlessness among pastoralists in case large tracts of land were allocated to individual ranchers, to avoid environmental degradation due to overstocking on communal lands, to establish a livestock production system that would allow modernisation or modification of livestock husbandry and still preserve many of the traditional ways of life without causing social frictions or an abrupt break with traditional ways of life. The group ranch concept was implemented through the Kenya Livestock Development Policy (KLDP) I and II(Ng'ethe, 1992). Despite this attempt to manage the rangelands, most of these group ranches are poorly managed.

In looking into the impact of livestock grazing on savannah grassland in Kenya, KIOKO et al., (2012) highlighted the importance of proper range management showing that continuous grazing has long term undesirable effects on rangeland, and impairs the functional characteristics of plants. Similar sentiments are also echoed by Angassa, (2014) from his findings that herbaceous species richness and abundance seems to decline under heavy grazing intensity. For efficient management of the rangelands, and to be able to discern and describe how rangelands are changing at multiple spatial and temporal scales the integration of sensors that possess specific characteristics is required.

2.3 Remote sensing and rangeland management

Remote sensing has created the unprecedented capacity to study the Earth by providing repeated measurements of biological and physical phenomena which offers a significant value to range management(Tueller, 1989). In the recent past, there have been dramatic improvements in data collection and availability, spatial and spectral resolution, and temporal frequency. enable greater discrimination of many biophysical and physical features. The continuous collection and utilization of land remote sensing data are of major benefit in studying and understanding human impacts on the environment, in managing the Earth's resources, in carrying out national security functions, and in planning and conducting many other activities of scientific, economic, and social importance. In rangeland management, remote sensing can be used in mapping rangeland fires, mapping biomass and assessment of vegetation health, determining rain use efficiency, computing net primary productivity (NPP), carrying out forage assessment, and analysing land use land cover change(Reeves et al., 2016).

The improvement in remote sensing data and technology has brought about remote sensing “Big Data”. The remote sensing ‘‘Big Data’’ not merely refers to the volume and velocity of data that outstrip storage and computing capacities, but also the variety and complexity of remote sensing data. There are several aspects and features of the remote sensing ‘‘Big Data’’ that include: the huge volume and rate of remote sensing data, the diversity of remote sensing data and also the complexity of remote sensing data especially the higher dimensionality brought about by remote sensing sensors and technologies customised for different earth science disciplines(Ma et al., 2015). It is almost impossible to handle remote sensing ‘‘Big Data’’ in a common workstation hence the need for a powerful computing tool such as Google Earth Engine.

2.4 Google Earth Engine

In 2008, after the USGS release of Landsat imagery, Google launched the cloud-based IDE (Integrated Development Environment) Google Earth Engine (GEE) to run the Earth Engine API (Application Program Interface). Google Earth Engine is a cloud-based platform that consists of a multi-petabyte analysis-ready data catalogue co-located with a high-performance, intrinsically parallel computation service. It is accessed and controlled through an Internet-accessible application programming interface (API) and an associated web-based interactive development environment (IDE) that enables rapid prototyping and visualization of results(Gorelick et al., 2017). JavaScript is the language of choice within this API. This does require the user to have a background in JavaScript as this is not a GUI platform.

GEE data is made up of Earth-observing remote sensing imagery, including the entire Landsat archive as well as complete archives of data from Sentinel-1 and Sentinel-2, but it also includes climate forecasts, land cover data and many other environmental, geophysical and socio-economic datasets. The catalogue is continuously updated at a rate of nearly 6000 scenes per day from active missions, with a typical latency of about 24 h from scene acquisition time. Users can request the addition of new datasets to the public catalogue, or they can upload their private data via a REST interface using either browser-based or command-line tools and share with other users or groups as desired Related images, such as all of the images produced by a single sensor,

are grouped and presented as a “collection”. The images are pre-processed to facilitate fast and efficient access (Gorelick et al., 2017).

The functions in the GEE library utilize several built-in parallelization and data distribution models such as image tiling, spatial aggregations, streaming collections, and caching and common sub-expression elimination to achieve high performance. This enables the calculation of derivatives to be performed in bulk and in parallel and data resolutions to be managed directly by the platform(Gorelick et al., 2017; Padarian, Minasny, & McBratney, 2015). It also contains a wide variety of classification models, and all the processing and computations are done on the fly which allows the computer to re-project and process data in close to real-time(Gorelick et al., 2017; Hansen et al., 2013; Padarian et al., 2015).

GEE has been used in a wide variety of research areas. In a demonstration study, Padarian, Minasny and McBratney, (2015) successfully show the ability of GEE to generate continuous soil prediction and classification of categorical data at a speed 40 – 100 times faster compared with conventional DSM using a desktop workstation. This sentiment is also echoed by Goldblatt *et al.*, (2016) when the carried out pixel-based image classification to map urban area boundaries in India. Patel *et al.*, (2015) also used GEE to map urban extent in an attempt to map a multi-temporal settlement and population, based on Normalized Difference Spectral Vector (NDSV). In their study, they demonstrate the ability to work with temporal data available in GEE environment.

Having a huge collection of temporal data and a faster computing power makes GEE a powerful tool for analysing land use land cover change. This is exploited by Nyland, Gunn, Shiklomanov, Engstrom, & Streletskiy, (2018) when they mapped land cover changes in the Lower Yenisei River region. There is hardly any work that has been done using GEE to monitor vegetation changes within rangeland areas globally not to mention Kenya, despite the huge potential. This study will be the first. We are going to use a similar method used by Huang et al., (2017) in mapping major land cover dynamics in Beijing.

CHAPTER 3: MATERIALS AND METHODS

3.1 Study Site

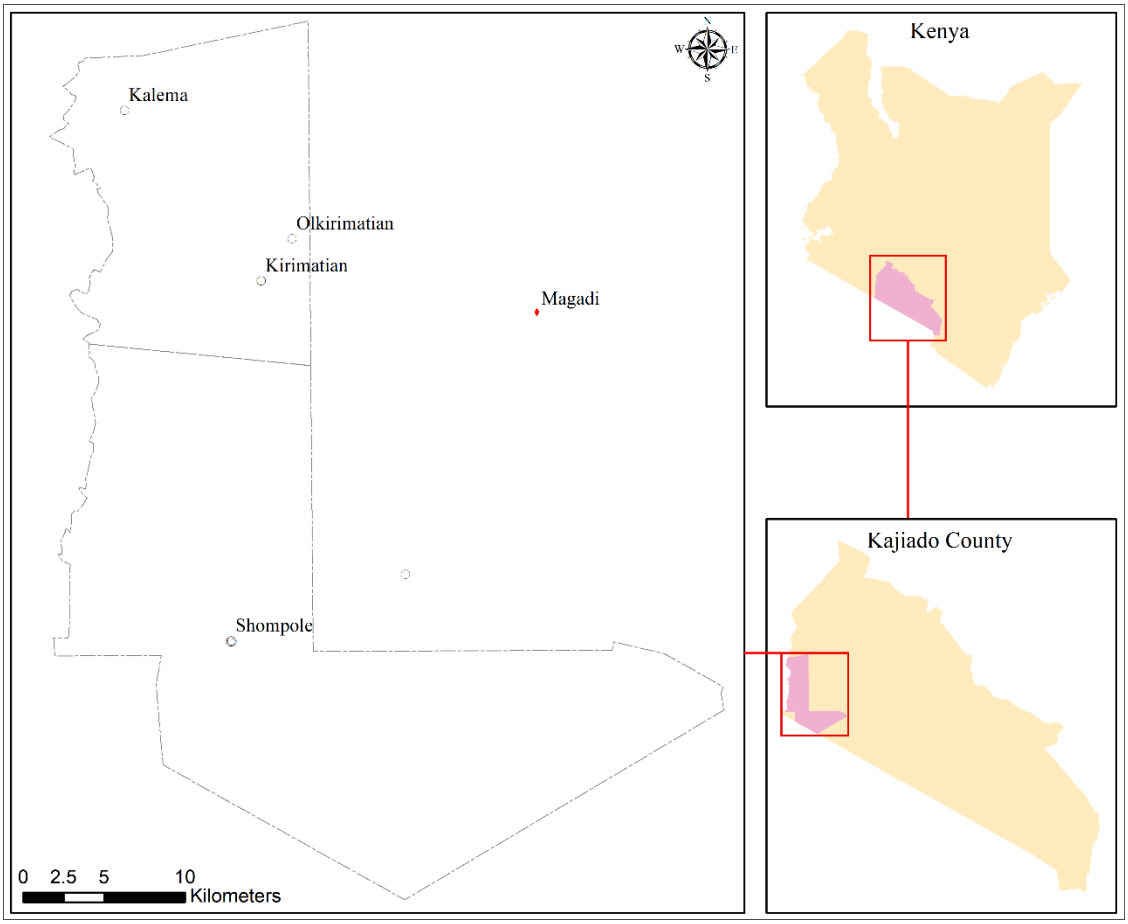

Figure 1: Map of the study area Olkirimatian and Shompole group ranches.

The study area, Shompole and Olkirimatian group ranches, are situated in Kajiado county, southern Kenya. The area has an altitude of 600–700m and high temperatures ranging from 18°C at night to 45°C during the day. The area is semi-arid, and rainfall is erratic and bimodal averaging 400-600 mm/ yr. A perennial river, the Ewaso Nyiro, bisects the area, providing an important source of water. The biophysical classification of the rangeland includes all those biomes found within and along the Ewaso Nyiro River, the shrubs and thickets between the Magadi Lake and the Nguruman Escarpment in the north and the Shompole hills in the south. There are swamps, like the Shompole swamp, which define the extent of the wet season grazing areas. The Shompole hills and Nguruman Escarpment provide the best areas for dry season grazing and wildlife conservation.

The Olkirimatian group ranch in Kajiado county occupies an area of 24,000 ha. While Shompole group ranch, adjacent to Olkirimatian, covers 62,700 ha. Both group ranches were established in 1979, and are mainly inhabited by the Maasai community who are pastoralists. The land under these group ranches is owned collectively by the group ranch members. The group ranches are run by an executive committee, the group ranch committee (GRC). The committee is composed of leaders elected by the community members. Under this committee, there are subcommittees or special tasks committees. They include the security committee, the conservation or natural resources management committee, and the investment committee. The customary institution of a council of elders also helps in guiding on certain issues, including dispute resolution. Major decisions on group ranch operation are made by the community members during the annual general meetings or group gatherings. Decisions made during these group meetings are implemented or enforced by the GRCs with the help of the special program committees. The polygons of the group ranches were obtained from the South Rift Association of Land Owners (SORALO). An association comprising 16 group ranches that helps the communities plan, govern and manage the ranches.

3.2 Data

The dominant land use in a group ranch is grazing while land cover comprises largely of grasslands and shrubs. The best way to analyse land use land cover changes will be through looking at the changes in the fractional canopy cover using Landsat images. This was done as follows.

3.2.1 Landsat Data

This study used both Landsat 7 and 8 images. For both satellites, images from Collection 1 that are in Tier 1 and calibrated to top-of-atmosphere (TOA) were used. The study focused on the period from 2000 to 2019. This period covers 5 years before the establishment of South Rift Association of Land Owners (SORALO) and the period covering SORALO's interventions to improve the conservation of biodiversity within the group ranches("SORALO | South Rift Association of Land Owners," n.d.). Therefore, images – free of cloud cover and cloud shadow - were selected for this period and for the months of March through June which covered the long rain period.

3.2.2 Gap filling

In May 2003, scan-line corrector (SLC) mechanism within the ETM+ for Landsat 7 satellite failed. This failure resulted in wedge-like features at both the eastern and the western edges of Landsat 7 images from May 2003(Williams, Goward, & Arvidson, 2006) (see figure 2 below). A neighbourhood similar pixel interpolator (NSPI) gap filling algorithm was used to correct Landsat 7 images. This method assumes that pixels closer to the pixel with missing data share similar spectral characteristics. In this, the pixels neighbouring the target pixel were first identified and their distance to the target pixel is computed. From there, similarity weights are computed and these weights are used to predict the radiometric value for the missing pixels(Asare, Forkuo, Forkuor, & Thiel, 2020). This gap filling method is faster compared to other method and the results are shown in figure 3 below.

Figure 2: Landsat image with SLC failure

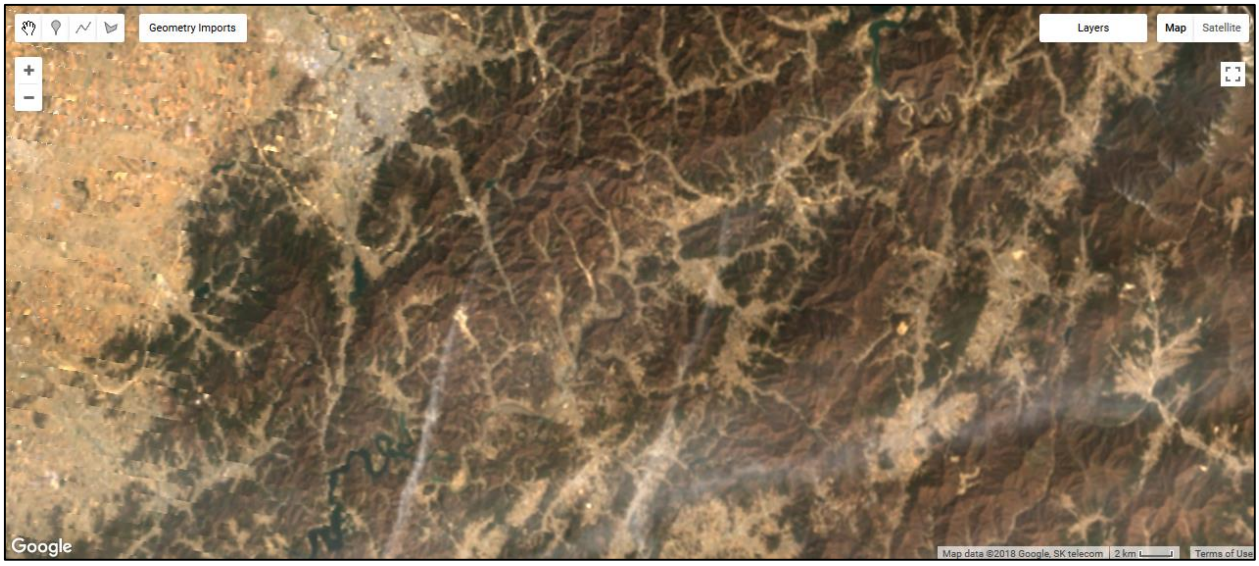

Figure 3: Landsat image corrected for SLC failure

3.2.3 Mosaicking

The study area was covered by three Landsat image tiles (path:169, row: 61; path: 168, row: 61; and path: 168, row: 62). The cloud-free images were mosaicked and then clipped by the polygon of the study area. In the end, 19 images were analysed each for each year starting from 2000 to 2019.

3.3 Methodology

3.3.1 Soil Adjusted Total Vegetation Index

Normal vegetation monitoring like Normalized Difference Vegetation Index (NDVI) and Leafe Area Index (LAI) do not capture senescent vegetation which dominates rangelands. To capture the senescent vegetation, Normalized Difference Senescent Vegetation Index (NDSVI) which uses the short wave infrared (SWIR) was computed then corrected for soil brightness to obtain Soil Adjusted Total Vegetation Index (SATVI) (see equation 1 below).

$$SATVI = \frac{SWIR - R}{SWIR + R + l} * (1 + l)$$

Equation 1: Computation of Soil Adjusted Total Vegetation Index (SATVI)

Where *SWIR* is the short wave infrared band (band 5 and 6 of Landsat 7 and 8 respectively), *R* is the red band (band 3 and 4 of Landsat 7 and 8 respectively) and *l* is the soil brightness correction factor taken to be 0.5

3.3.2 Total Vegetation Fractional Canopy Cover (TVFC)

TVFC cover was computed using the formula shown in equation 2 below. *SATVI_Max* and *SATVI_Min* were obtained by computing SATVI layer for each year, the SATVI layers were then stacked together and the maximum and the minimum pixel values extracted from the stack respectively.

$$TVFC = \frac{SATVI - SATVI\_Min}{SATVI\_Max - SATVI\_Min} * 100$$

Equation 2: Computation of Total Vegetation Fractional Canopy (TVFC) Cover

Changes in TVFC cover were computed by calculating the difference between $TVFC_{2000}$ and $TVFC_{2005}$, $TVFC_{2005}$ and $TVFC_{2010}$, and $TVFC_{2010}$ and $TVFC_{2019}$. And areas with more than one standard deviation of the average difference were considered as areas with significant changes.

3.4 Tools

3.4.1 Google Earth Engine platform

The analysis was carried out using the GEE code editor which required login credentials. The login credentials can be obtained by sending a request to Google. The request is always processed within two days after which, one is given access to GEE platform. As GEE does not have a graphic user interface, data preparation and analysis was done using Javascript. Landsat images used were loaded from database linked to the code editor while the study area shapefile was uploaded. As

shown in the figure 4 below, the GEE platform has got various panels to load data, run a script and present the results.

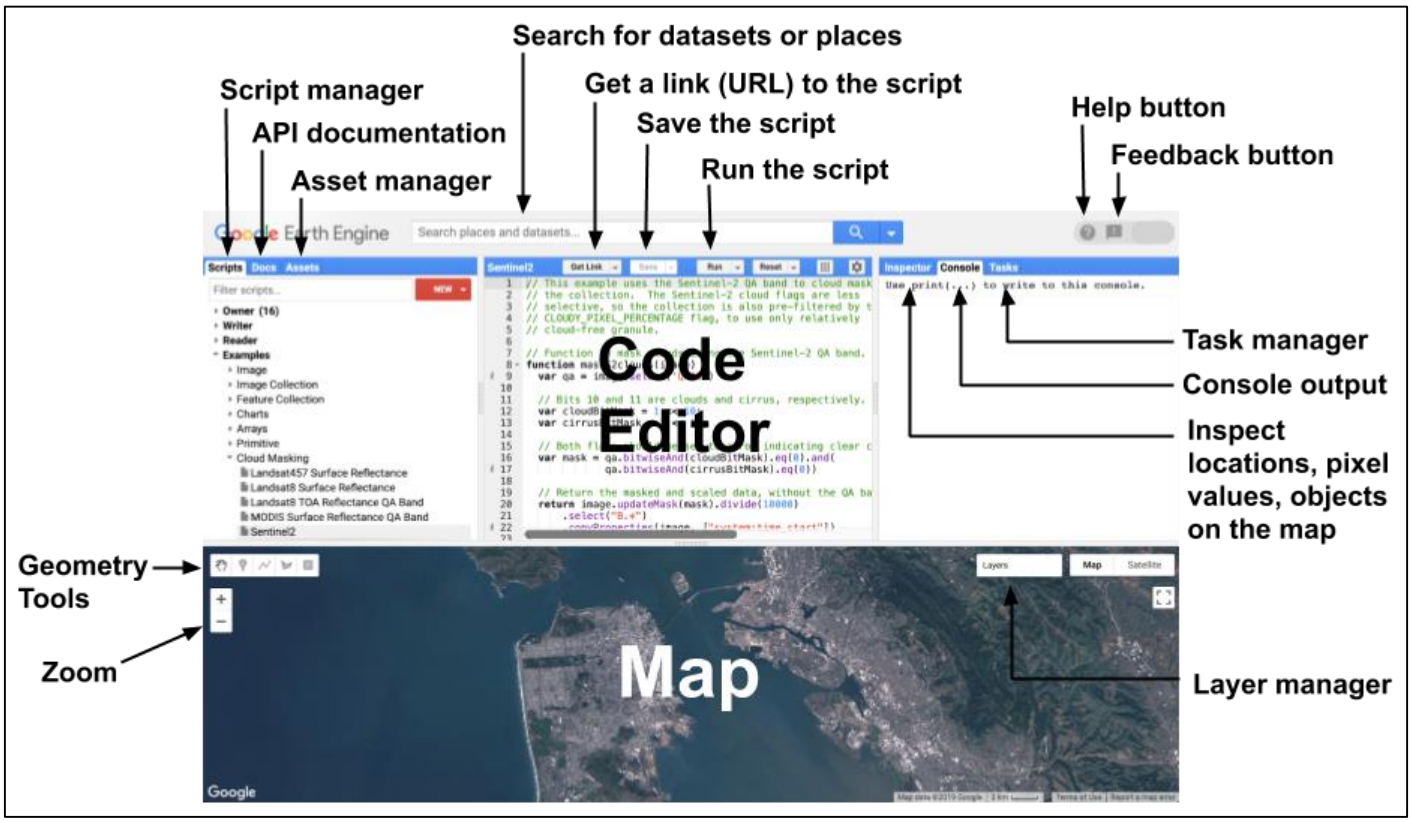

Figure 4: Google Earth Engine platform

3.4.2 ArcGIS

As it was cumbersome to produce publication maps using GEE platform. The maps presented in this report were prepared using ArcGIS 10.6 using a student license.

CHAPTER 4: RESULTS AND DISCUSSION

4.1 Results

4.1.1 Total Vegetation Fractional Canopy Cover

The study was able to map TVFC cover for the two group ranches for each epoch. Figure 5, 6, 7, and 8 show TVFC cover for 2000, 2005, 2010 and 2019 respectively. This was made possible by mosaicking cloud-free Landsat images captured between March and June. This period captures both the pick of a rainy season (April – characterised by high cloud cover) and the beginning of the dry season (June - characterised by low cloud cover) which is important for observing grassland and shrubland vegetation that dry's faster than woody vegetation.

The mosaicked Landsat images are composites of both green vegetation and senescent vegetation. Thus SWIR band was used for it's sensitive to water, which makes it have a higher reflectance as vegetation dries, instead of using NIR band commonly used for NDVI. Unfortunately, SWIR band also has a high reflectance for soil hence SATVI was computed by correcting for soil brightness.

While SATVI has a minimum value of 0.0, it does not have a maximum value, thus TVFC was computed using the overall minimum and overall maximum SATVI of the study period within the group ranches. This resulted in TVFC cover where areas without any vegetation get a value of 0 while areas with the maximum vegetation within the period get a value of 100.

From all the epochs, Shompole appeared to have a higher TVFC cover than Olkirimatian. Higher TVFC cover was observed in areas within and around the swamp and areas within and around the farming village (Kalema village). While lower TVFC cover was observed at the north-eastern parts of Olkirimatian that were characterised with sparse vegetation and baresoil. The lowest TVFC cover was observed at the shore of Lake Natron southwestern parts of Shompole group ranch. The observed TVFC cover ranged from 0 to about 50 which is common for semi-arid rangelands.

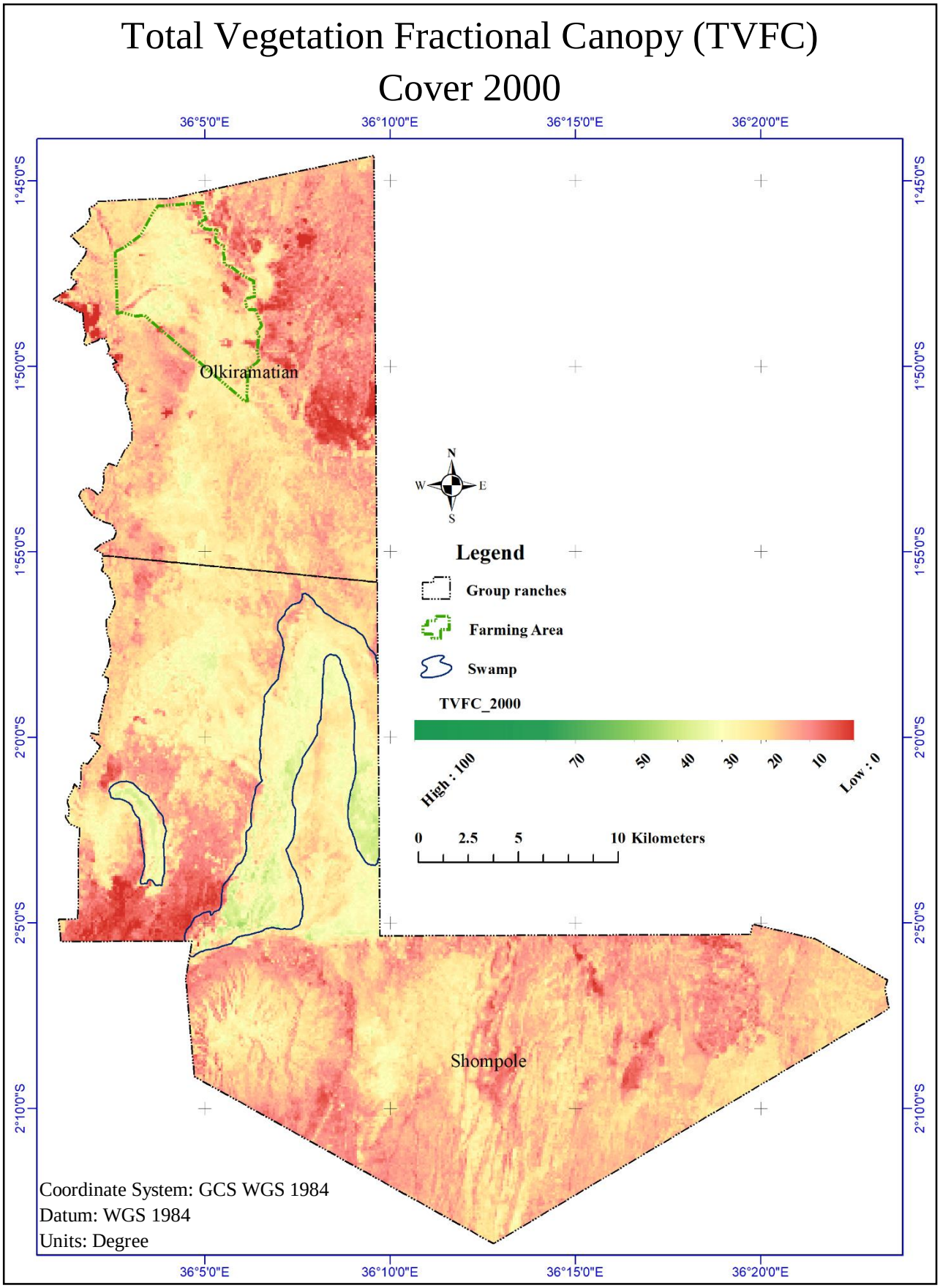

Figure 5: Total vegetation fractional canopy (TVFC) cover 2000

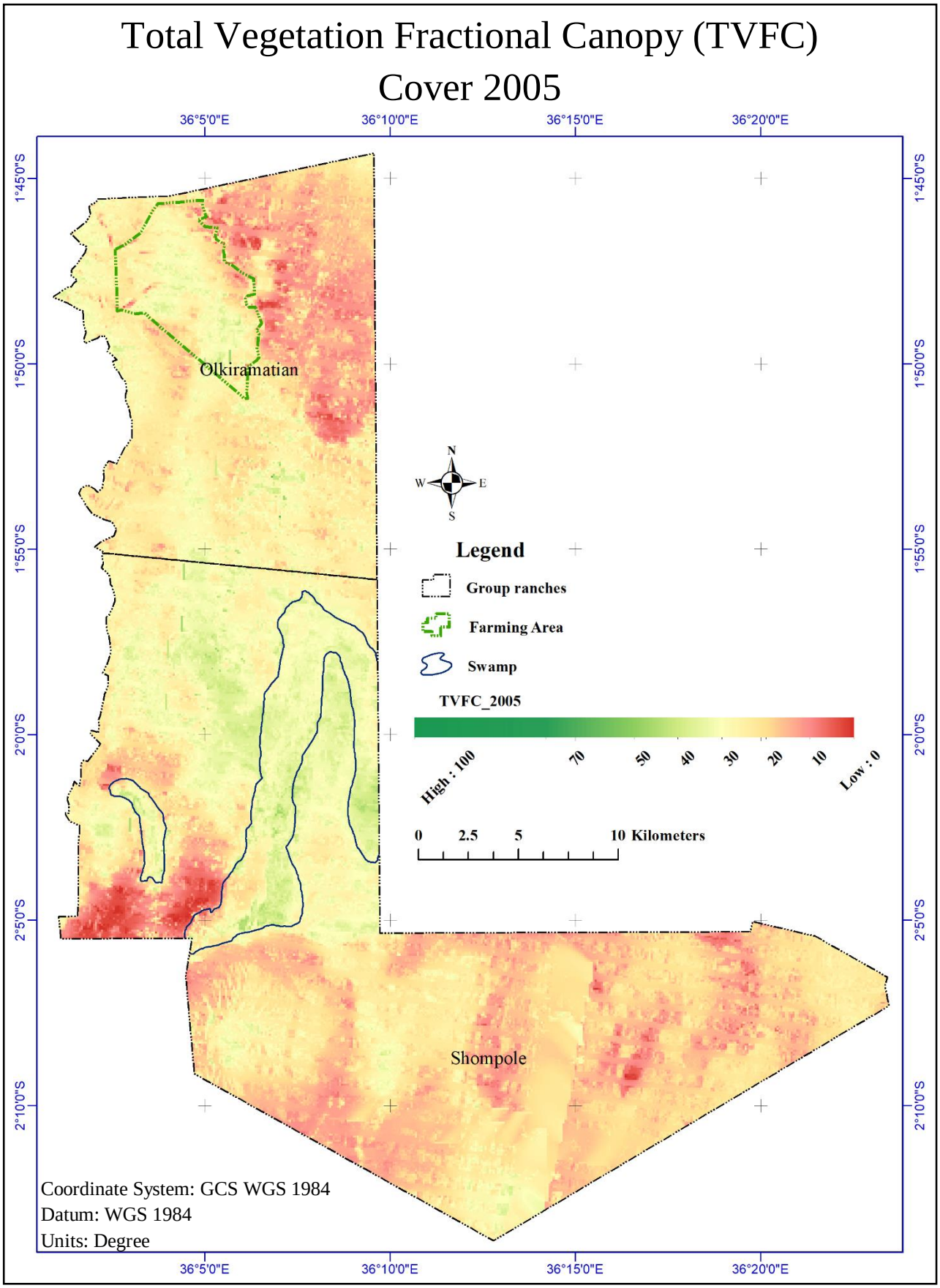

Figure 6: Total vegetation fractional canopy (TVFC) cover 2005

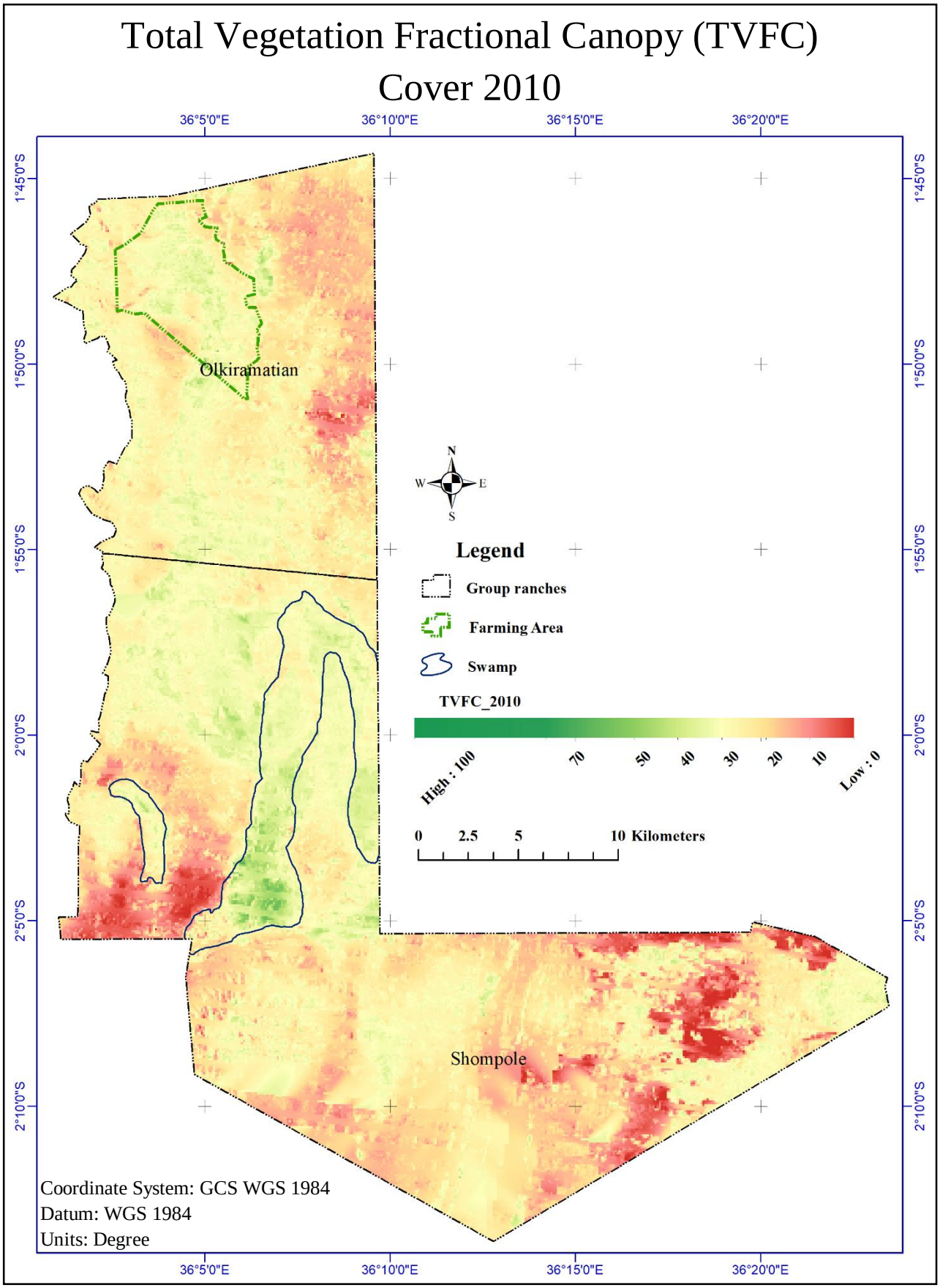

Figure 7: Total vegetation fractional canopy (TVFC) cover 2010

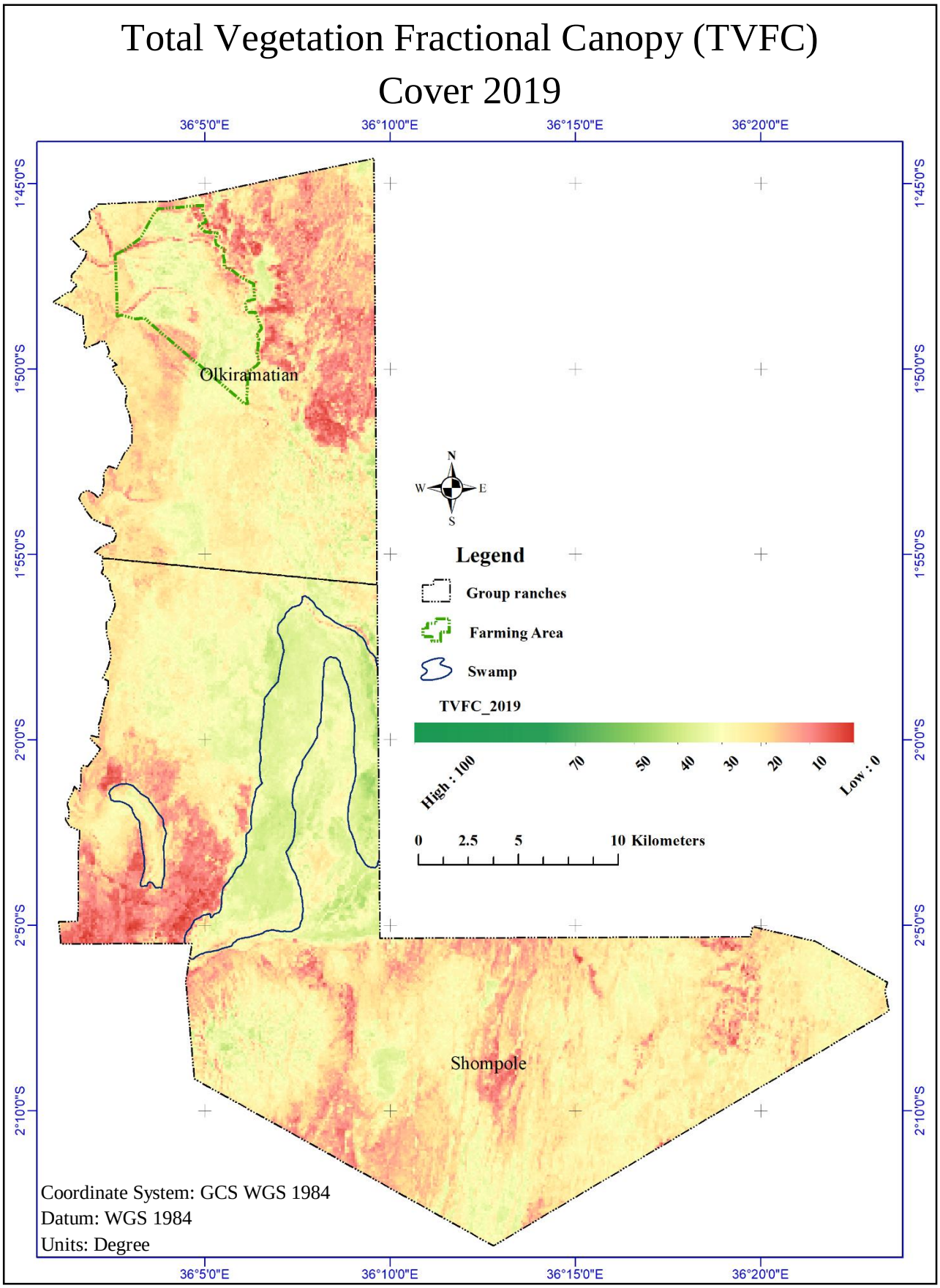

Figure 8: Total vegetation fractional canopy (TVFC) cover 2019

4.1.2 Changes in Total Vegetation Fractional Canopy Cover

By visual comparison of the TVFC cover maps, the has been a consistent increase of TVFC cover from the year 2000. Much of the increase was observed between 2000 and 2005 shown in figure 9, with an average increase of 4.5% (5.4 standard deviation) (see table 1 below). The increase in TVFC cover was distributed equally across the study area except for the southern part of the swamp that witnessed a decline in TVFC cover.

The period between 2005 and 2010 slight increase in TVFC cover compared (mean: 1.6%; standard deviation: 6.6) to the 2000-2005 period. Most of the increase occurred in Olkirimatian while in Shompole increase was only witnessed in areas around the swamp as seen in figure 10. Generally, more areas in Shompole had a decline in TVFC cover.

2010 to 2019 saw a general decline in TVFC cover with the whole area experiencing a decline of about 0.03% (with 7.0 standard deviation). The decline was observed more in Olkirimatian than Shompole, with Shompole having patches of TVFC cover increases. Some of the areas that saw some increases were the eastern part of the swamp and the southern parts of Oloika hill (see figure 11 below).

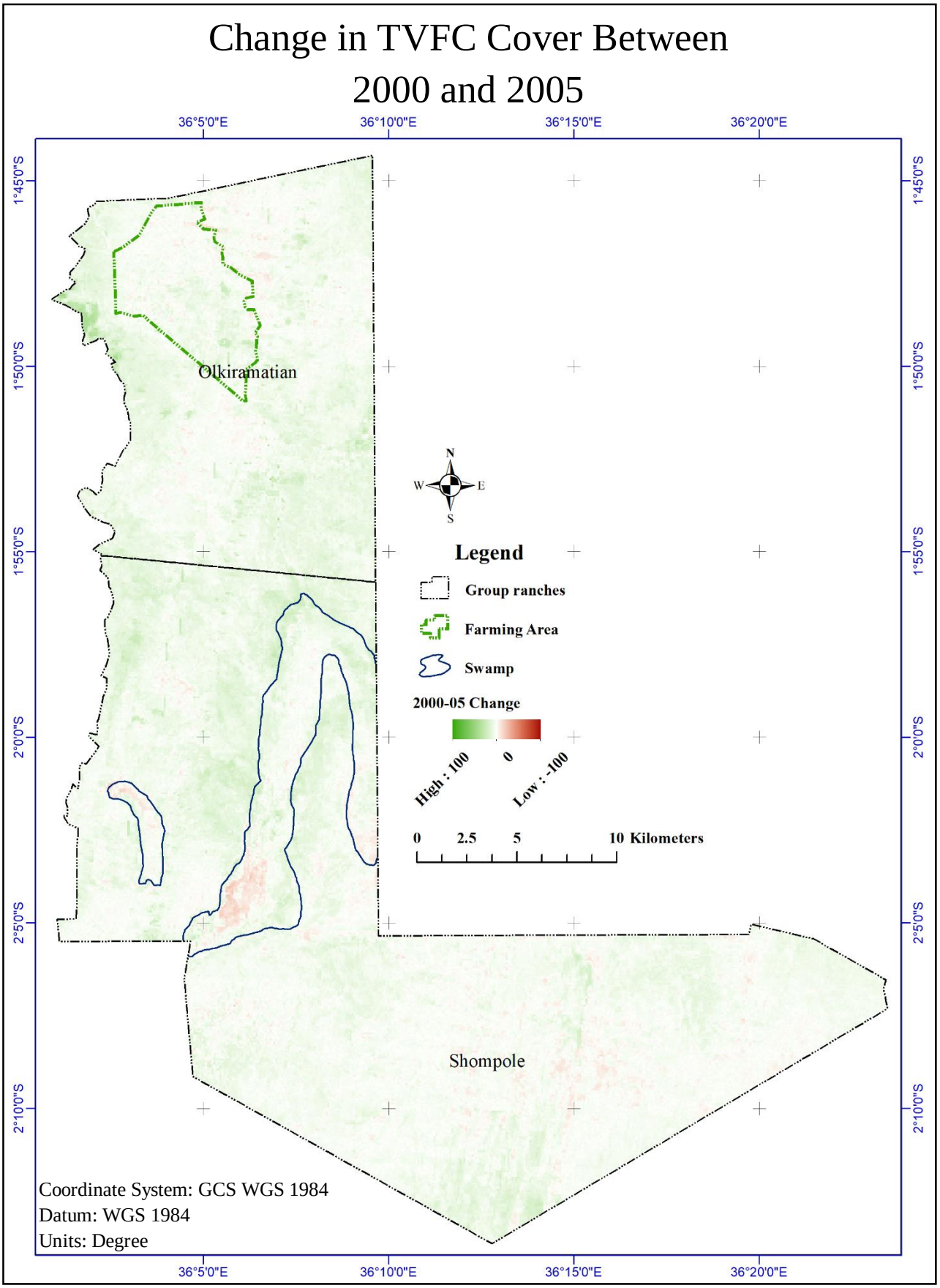

Figure 9: Change in TVFC cover between 2000 and 2005

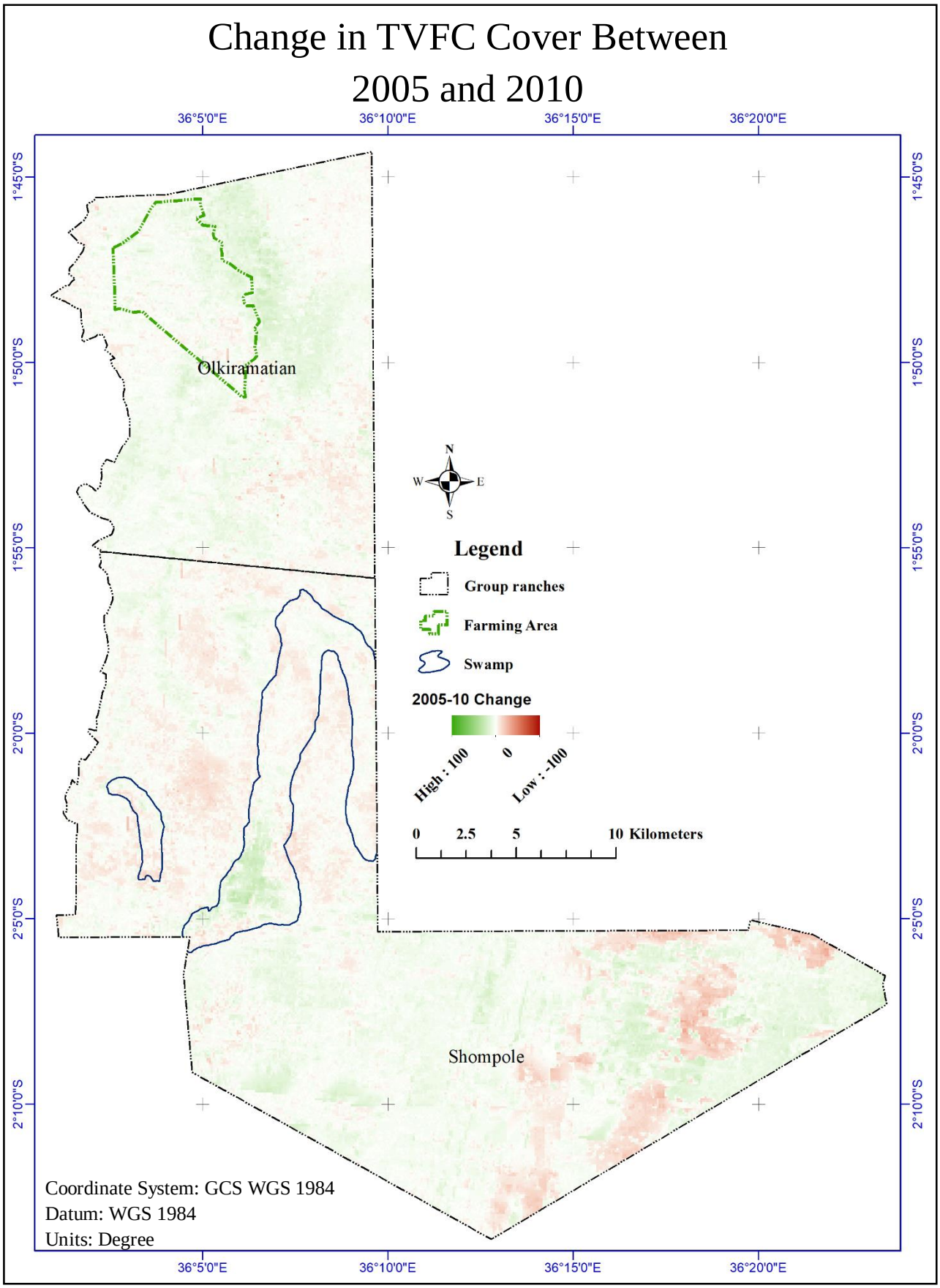

Figure 10: Change in TVFC cover between 2005 and 2010

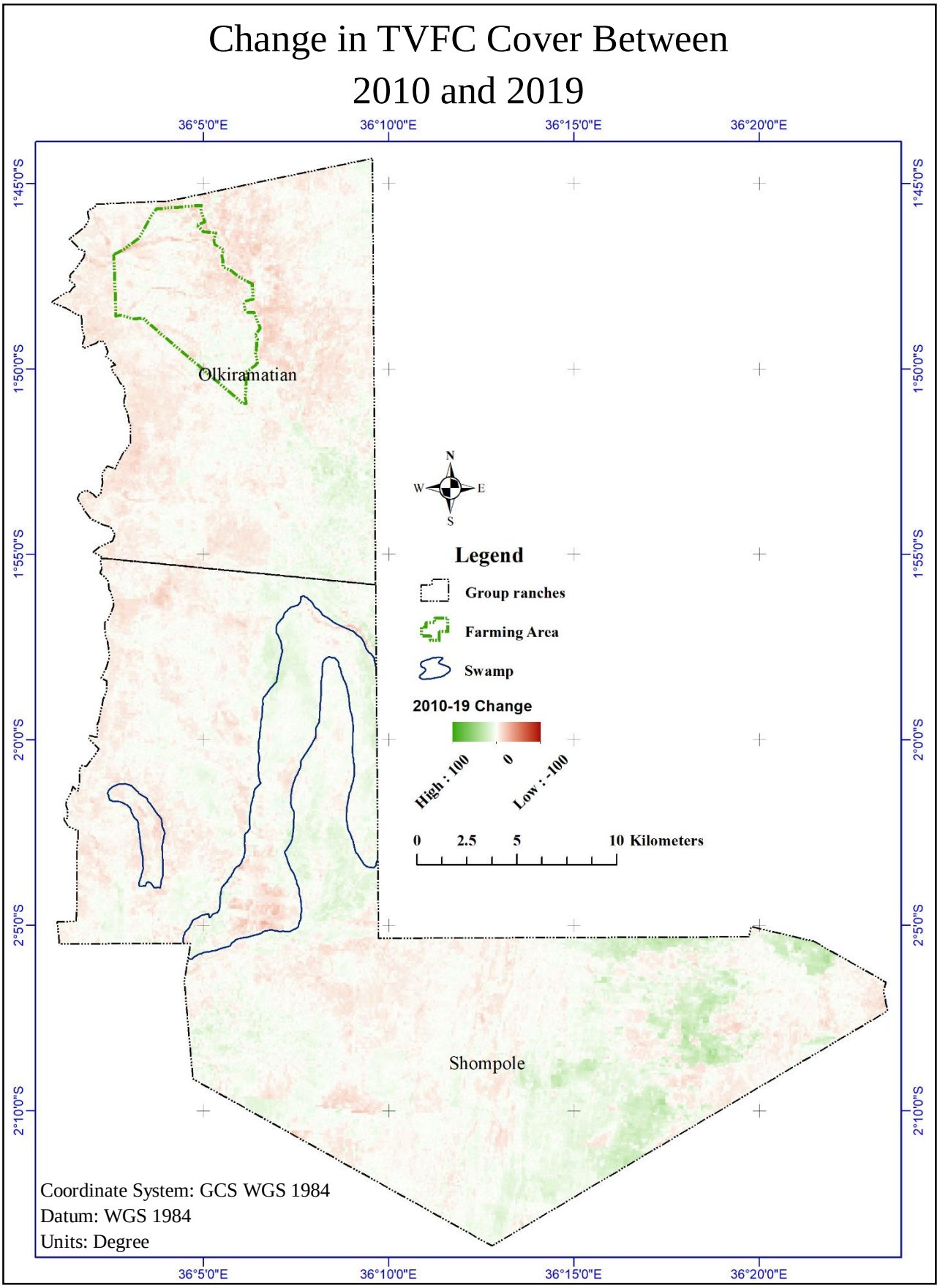

Figure 11: Change in TVFC cover between 2010 and 2019

Table 1: Mean and standard deviation of change in TVFC cover

	TVFC 2005-00	***TVFC 2010-05***	***TVFC 2019-10***
Mean	4.5261	1.6053	-0.0368
Standard deviation	5.3557	6.6041	7.0147

4.1.3 Total Vegetation Fractional Canopy Cover Gain

From 2000 to 2005 what was considered a significant increase on TVFC cover is shown in figure 12 to have occurred in the regions bordering the swamp and on the western border of both Olkirimatian and Shompole. This period saw significant TVFC cover gained in 1,250,620 pixels at a resolution of 10m (see table 2 below), the highest during the study period.

Significant TVFC cover gained between 2005 and 2010 was observed to the eastern sides of Kalema farming village, the southern border of Shompole swamp and at the southern edges of Shompole Group Ranch (see figure 13 below). The number of pixels that had significant TVFC cover gain were 1,048,812 pixels (at a resolution of 10m), the lowest during the study period.

For the period between 2010 and 2019, significant TVFC cover gain was observed to the eastern and south-eastern parts of Shompole and Olkirimatian Group Ranches respectively (see figure 14 below). The number of pixels with significant gain were 1,092,798 pixels, slightly higher than the period between 2005 and 2010.

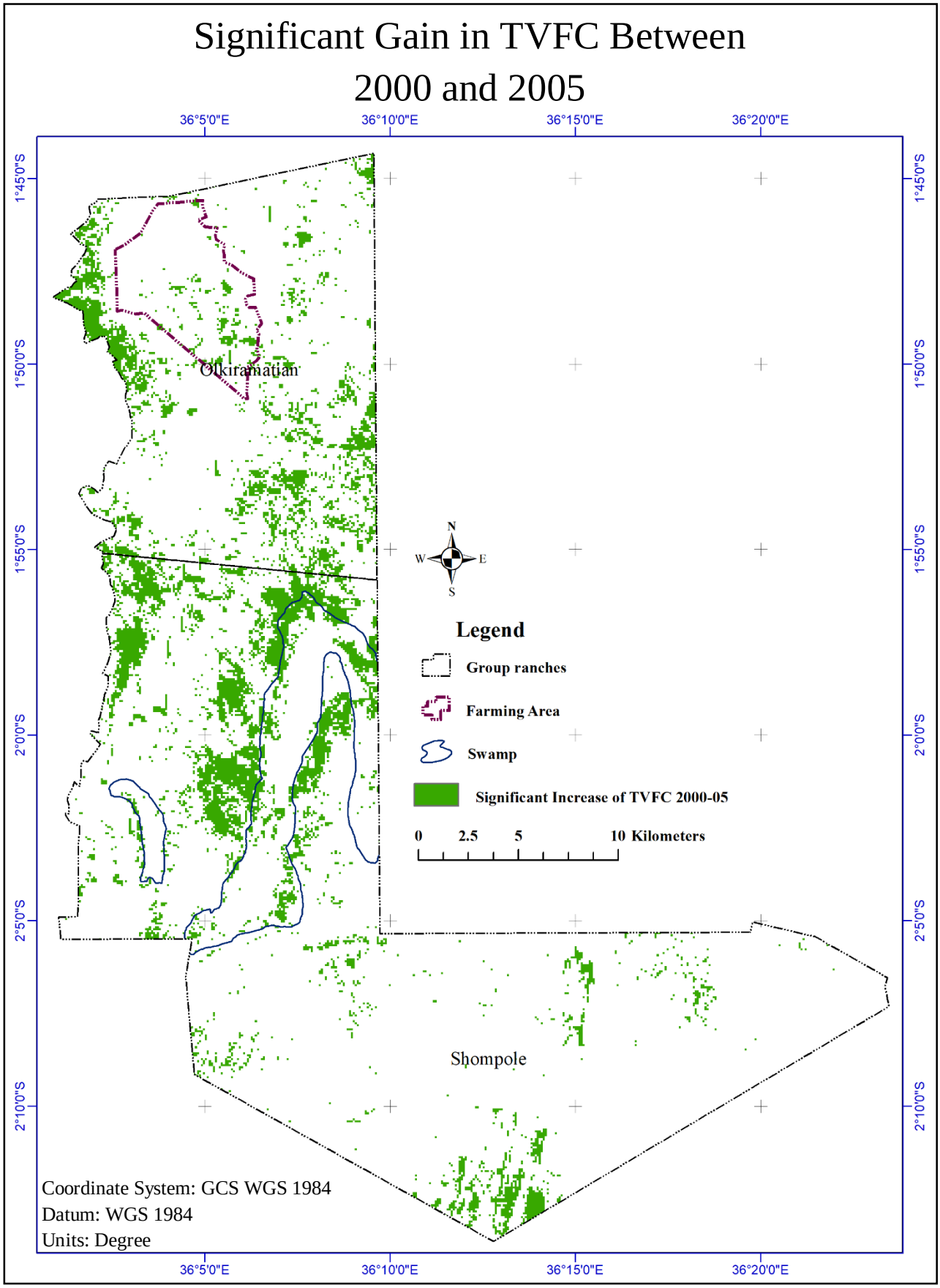

Figure 12: Significant gain in TVFC between 2000 and 2005

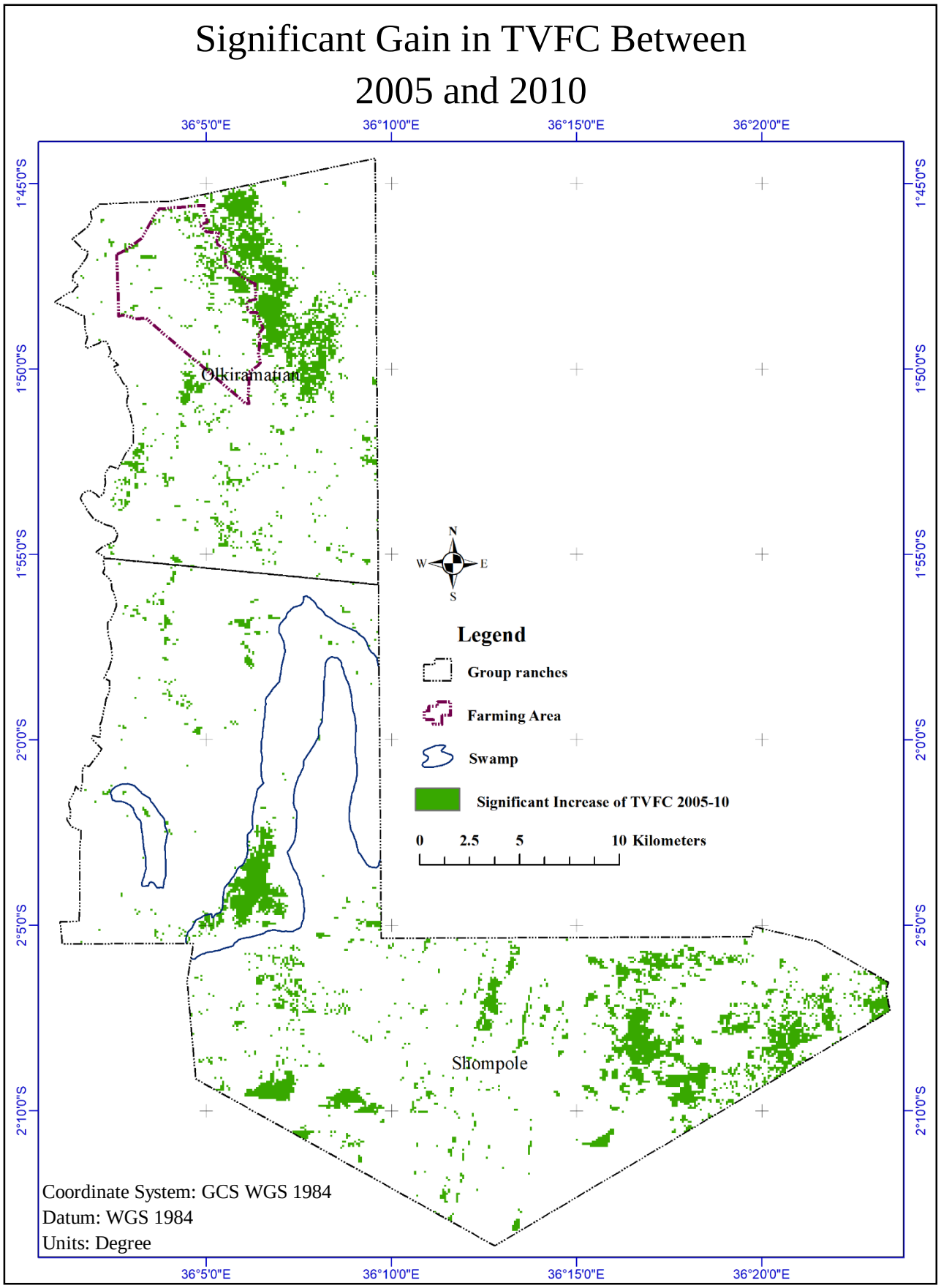

Figure 13: Significant gain in TVFC between 2005 and 2010

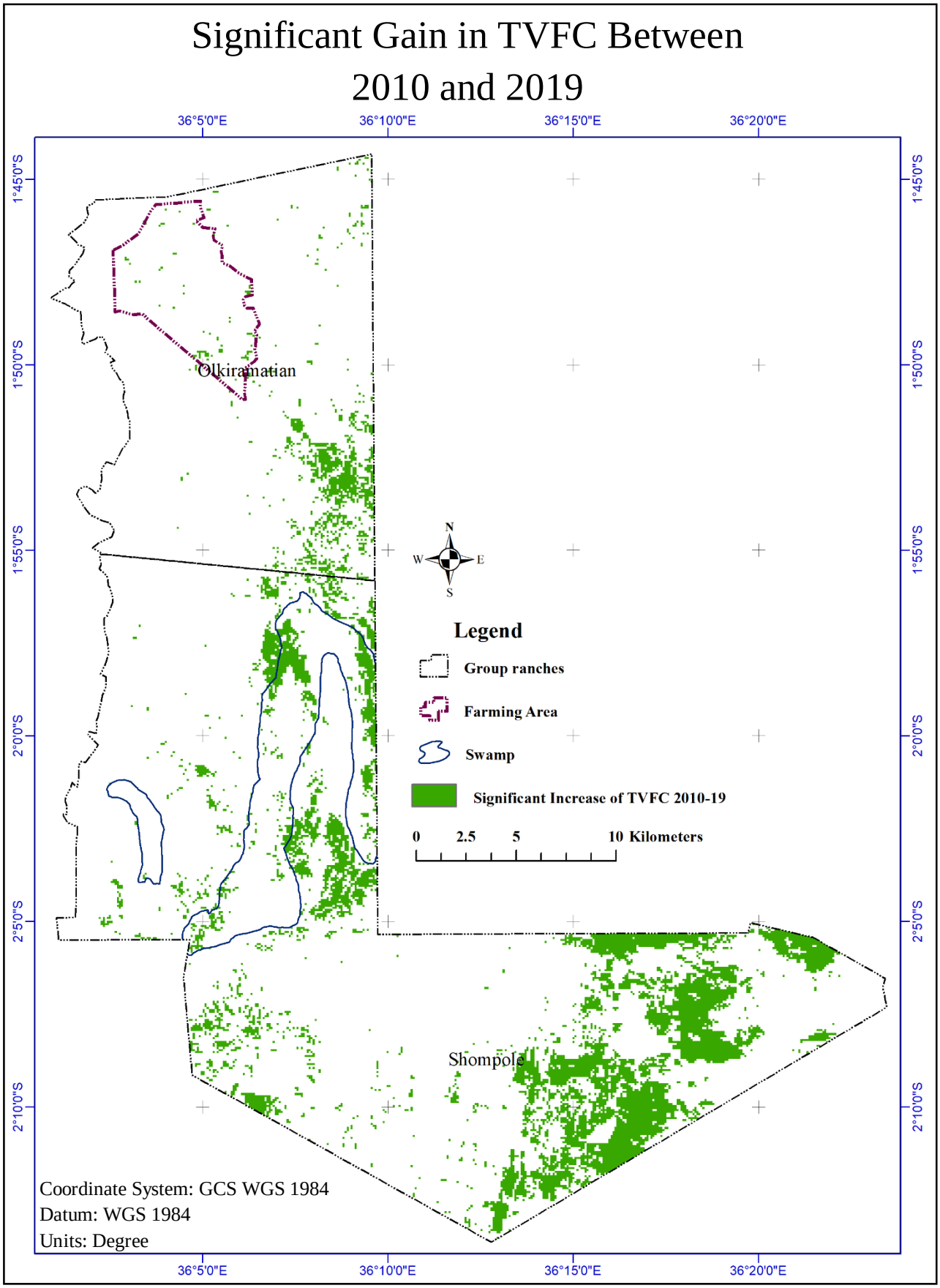

Figure 14: Significant gain in TVFC between 2010 and 2019

Table 2: Pixels with significant gain in TVFC cover at 10m spatial resolution

Time period	***Pixels with significant gain in TVFC***
2000-05	1,250,621
2005-10	1,048,812
2010-19	1,092,799

4.2 Discussion

In this study, GEE capabilities were utilised to monitor TVFC cover over two group ranches. The study used Landsat 7 and 8 images already available within the GEE database. The images had already been georeferenced thus saving time for analysis that would have been used downloading and georeferencing the images. With the minimum requirement of computing space and software, and with the continuous availability of Landsat 8 images this kind of monitoring can be employed on a near real-time if not on a monthly basis thus helping in understanding the changes in rangeland conditions.

Using TVFC cover to monitor rangelands cover gives the true picture of the rangelands, their health and their sustainability as it captures both green and senescent vegetation. Both of which provide forage to both livestock and wildlife animals. Computation of TVFC cover and TVFC cover changes involve a large number of pixels which takes time computing in a normal remotesesing system. This has been reduced to a few seconds working in the GEE environment. As the study was carried out during the long rainy season which also covers the planting season, the area encroached by farmers around Kalema village was conspicuously visible as it remained with high TVFC cover all through the study period. This is a clear indication of farming activities with Olkirimatian Group Ranch.

By computing the significant changes, this study was able to capture the shifting of the Shompole swamp between the western and the eastern arms of the swamp. In 2000 and 2010 the swamp was dominant on the western arm while in 2005 and 2019, it was dominant on the eastern arm. This shifting of the swamp is also documented by Lambin (2001).

While two out of three computations showing the changes in TVFC cover were observed in this study to have an average positive change, the negative change (2010 to 2019) was close to zero

which suggested that the two group ranches were either improving or remaining the same. A huge increase in TVFC cover was also observed in the change computation between 2000 and 2005. This coincided with the establishment of SORALO in 2005. These two observations support the claims that the interventions provided by SORALO are bearing fruits.

4.3 Study Limitations

While neighbourhood similar pixel interpolator (NSPI) gap filling algorithm was used to correct for SLC failure, the algorithm was not very efficient as strip-like features were still visible when the images were zoomed. This might have introduced errors in the computation. However, since the study captured a huge area, the error introduced was very negligible.

CHAPTER 5: CONCLUSION AND RECOMMENDATION

5.1 Conclusion

Rangeland ecosystems are important to the pastoral communities and harnessing their full potential remain a challenging desire. In this study, using GEE platform to monitor TVFC cover has been demonstrated to be a useful tool that can be adopted for rangeland management. Once the script has been developed, it takes a short time to execute. The script also requires very little modification to be implemented for different areas and time period hence can be used to compare different scenes. With these capabilities, GEE platform can be employed in the planning of grazing patterns - by monitoring seasonal or monthly changes of TVFC cover, or to highlighting the impacts of climate change and anthropogenic activities - by monitoring annual TVFC cover changes.

By monitoring the changes in TVFC cover, the study detects some land cover land-use changes in the study area. The study shows that there is an increase in vegetation within the group ranches which is a move in the right direction as the increase in vegetation translate to increase in forage for the pastoral communities living within the group ranches.

5.2 Recommendation

While the TVFC cover was vital in showing changes in both green and senescent vegetation, this method should be complemented with fieldwork to identify the main causes of TVFC cover changes. Fieldwork will help identify illegal farming activities responsible for increasing TVFC cover, and the extent of events such as wildfires that are responsible for reducing TVFC cover.

While the study showed areas with significant TVFC cover gain, the same analysis should be carried to map areas with significant TVFC cover loss. A map of areas with significant TVFC cover loss highlights areas that require new interventions strategies or areas that call for further investigations.

Recently, rangelands have witnessed an increase in invasive plant species. Some of these new invasive vegetation is capable of colonising rangelands to the extent that useful forage cannot regrow. It is therefore important to use optical images (Landsat images in this case) together with

Synthetic Aperture Radar (SAR) images (such as Sentinel-1) that are capable of detecting the structure and composition of the vegetation.

APPENDICES

Appendix A: JavaScript Code

```
// load area of interest
Var aoi: Table user/oloostephen08/OlSho
// load Landsat 8 TOA reflectances, terrain corrected.
var l8toa = ee.ImageCollection('LANDSAT/LC08/C01/T1_TOA').filterBounds(aoi);
// load Landsat 7 TOA reflectances, terrain corrected.
var l7toa = ee.ImageCollection("LANDSAT/LE07/C01/T1_TOA")
.filterBounds(aoi);
//////////////////////////////////////////////////////////////////////////////
// Layer preparation
//
// Functions to obtain landsat image with minimum cloud cover
// Landsat 8
var maskClouds = function(l8toa) {
var scored = ee.Algorithms.Landsat.simpleCloudScore(l8toa);
return l8toa.mask(scored.select(['cloud']).lt(25));
};
//
// Landsat 7
var maskClouds2 = function(l7toa) {
var scored = ee.Algorithms.Landsat.simpleCloudScore(l7toa);
return l7toa.mask(scored.select(['cloud']).lt(25));
};
//
// This function to compute Soil Adjusted Vegetation Index (SATVI)
// Landsat 8
var addQualityBands = function(l8toa) {
 var one = ee.Image(1);
 return maskClouds(l8toa)
 // Soil Adjusted Total Vegetation Index (SATVI)
 .addBands(l8toa.expression("(((b6 - b4) / (b6 + b4 + 0.5)) * (1 + 0.5)) - (b7 / 2)", {
    b7: l8toa.select("B7"),
    b6: l8toa.select("B6"),
    b4: l8toa.select("B4")
}).rename('satvi'))
 .addBands(l8toa.metadata('system:time_start'))
 .addBands(one.divide(l8toa.metadata('CLOUD_COVER')).rename('inv_cloudiness'));
};

// Landsat 7
var addQualityBands2 = function(l7toa) {
```

```
 var one = ee.Image(1);
 return maskClouds2(l7toa)
// Soil Adjusted Total Vegetation Index (SATVI)
 .addBands(l7toa.expression("(((b5 - b3) / (b5 + b3 + 0.5)) * (1 + 0.5)) - (b7 / 2)", {
    b7: l7toa.select("B7"),
    b5: l7toa.select("B5"),
    b3: l7toa.select("B3")
}).rename('satvi'))
 .addBands(l7toa.metadata('system:time_start'))
 .addBands(one.divide(l7toa.metadata('CLOUD_COVER')).rename('inv_cloudiness'));
};

//Determining the minimum amd maximum SATVI

//Selecting images that fit our requirements for the min max
var l7toa0012 = l7toa.filterDate('2000-02-15', '2012-06-15')
.map(addQualityBands2);

//Creating the composite for the min max
var l7toa0012_satvi = l7toa0012.qualityMosaic('satvi');


// Computation of minimum and maximu SATVI
// This is done for the whole study period

var max = l7toa0012_satvi.select(['satvi']).reduceRegion({
  reducer: ee.Reducer.max(),
  geometry: aoi.geometry(),
  crs: 'EPSG:4326',
  scale: 30,
  maxPixels: 1e9
});

var min = l7toa0012_satvi.select(['satvi']).reduceRegion({
  reducer: ee.Reducer.min(),
  geometry: aoi.geometry(),
  crs: 'EPSG:4326',
  scale: 30,
  maxPixels: 1e9
}); // end of min max computation

//print(min);
//print(max);

// Selecting images that fit our requirements
// For Landsat 7 we carried out gap filling from the year 2004 t0 2012
```

```
var l7toa2000 = l7toa.filterDate('2000-02-15', '2000-06-15').map(addQualityBands2);
var l7toa2001 = l7toa.filterDate('2001-02-15', '2001-06-15').map(addQualityBands2);
var l7toa2002 = l7toa.filterDate('2002-02-15', '2002-06-15').map(addQualityBands2);
var l7toa2003 = l7toa.filterDate('2003-02-15', '2003-06-
15').map(addQualityBands2).map(function(image){
  var filled1a = image.focal_mean(2, 'square', 'pixels', 32);
  return filled1a.blend(image)});
var l7toa2004 = l7toa.filterDate('2004-02-15', '2004-06-
15').map(addQualityBands2).map(function(image){
  var filled1a = image.focal_mean(2, 'square', 'pixels', 32);
  return filled1a.blend(image)});
var l7toa2005 = l7toa.filterDate('2005-02-15', '2005-06-
15').map(addQualityBands2).map(function(image){
  var filled1a = image.focal_mean(2, 'square', 'pixels', 8);
  return filled1a.blend(image)});
var l7toa2006 = l7toa.filterDate('2006-02-15', '2006-06-
15').map(addQualityBands2).map(function(image){
  var filled1a = image.focal_mean(2, 'square', 'pixels', 32);
  return filled1a.blend(image)});
var l7toa2007 = l7toa.filterDate('2007-02-15', '2007-06-
15').map(addQualityBands2).map(function(image){
  var filled1a = image.focal_mean(2, 'square', 'pixels', 32);
  return filled1a.blend(image)});
var l7toa2008 = l7toa.filterDate('2008-02-15', '2008-06-
15').map(addQualityBands2).map(function(image){
  var filled1a = image.focal_mean(2, 'square', 'pixels', 32);
  return filled1a.blend(image)});
var l7toa2009 = l7toa.filterDate('2009-02-15', '2009-06-
15').map(addQualityBands2).map(function(image){
  var filled1a = image.focal_mean(2, 'square', 'pixels', 32);
  return filled1a.blend(image)});
var l7toa2010 = l7toa.filterDate('2010-02-15', '2010-06-
15').map(addQualityBands2).map(function(image){
  var filled1a = image.focal_mean(2, 'square', 'pixels', 8);
  return filled1a.blend(image)});
var l7toa2011 = l7toa.filterDate('2011-02-15', '2011-06-
15').map(addQualityBands2).map(function(image){
  var filled1a = image.focal_mean(2, 'square', 'pixels', 32);
  return filled1a.blend(image)});
var l7toa2012 = l7toa.filterDate('2012-02-15', '2012-06-
15').map(addQualityBands2).map(function(image){
  var filled1a = image.focal_mean(2, 'square', 'pixels', 32);
  return filled1a.blend(image)});

var l8toa2013 = l8toa.filterDate('2013-02-15', '2013-06-15').map(addQualityBands);
var l8toa2014 = l8toa.filterDate('2014-02-15', '2014-06-15').map(addQualityBands);
```

```
var l8toa2015 = l8toa.filterDate('2015-02-15', '2015-06-15').map(addQualityBands);
var l8toa2016 = l8toa.filterDate('2016-02-15', '2016-06-15').map(addQualityBands);
var l8toa2017 = l8toa.filterDate('2017-02-15', '2017-06-15').map(addQualityBands);
var l8toa2018 = l8toa.filterDate('2018-02-15', '2018-06-15').map(addQualityBands);
var l8toa2019 = l8toa.filterDate('2019-02-15', '2019-06-15').map(addQualityBands);

//Creating the composite
var l7toa2000_satvi = l7toa2000.qualityMosaic('satvi');
var l7toa2001_satvi = l7toa2001.qualityMosaic('satvi');
var l7toa2002_satvi = l7toa2002.qualityMosaic('satvi');
var l7toa2003_satvi = l7toa2003.qualityMosaic('satvi');
var l7toa2004_satvi = l7toa2004.qualityMosaic('satvi');
var l7toa2005_satvi = l7toa2005.qualityMosaic('satvi');
var l7toa2006_satvi = l7toa2006.qualityMosaic('satvi');
var l7toa2007_satvi = l7toa2007.qualityMosaic('satvi');
var l7toa2008_satvi = l7toa2008.qualityMosaic('satvi');
var l7toa2009_satvi = l7toa2009.qualityMosaic('satvi');
var l7toa2010_satvi = l7toa2010.qualityMosaic('satvi');
var l7toa2011_satvi = l7toa2011.qualityMosaic('satvi');
var l7toa2012_satvi = l7toa2012.qualityMosaic('satvi');

var l8toa2013_satvi = l8toa2013.qualityMosaic('satvi');
var l8toa2014_satvi = l8toa2014.qualityMosaic('satvi');
var l8toa2015_satvi = l8toa2015.qualityMosaic('satvi');
var l8toa2016_satvi = l8toa2016.qualityMosaic('satvi');
var l8toa2017_satvi = l8toa2017.qualityMosaic('satvi');
var l8toa2018_satvi = l8toa2018.qualityMosaic('satvi');
var l8toa2019_satvi = l8toa2019.qualityMosaic('satvi');

////////////////////////////////////////////////////////////////////////////////
//
//Computation of the total fractional vegetation cover
//
var tvfc_2000 = l7toa2000_satvi.expression(
  '((satvi - (-0.02318617898610694)) / (0.612232341133361 - (-0.02318617898610694))) * 100',
{
    'satvi': l7toa2000_satvi.select('satvi')
    }).rename('tvfc');

var tvfc_2001 = l7toa2001_satvi.expression(
  '((satvi - (-0.02318617898610694)) / (0.612232341133361 - (-0.02318617898610694))) * 100',
{
    'satvi': l7toa2000_satvi.select('satvi')
    }).rename('tvfc');

var tvfc_2002 = l7toa2002_satvi.expression(
```

```
  '((satvi - (-0.02318617898610694)) / (0.612232341133361 - (-0.02318617898610694))) * 100',
{
    'satvi': l7toa2002_satvi.select('satvi')
    }).rename('tvfc');

var tvfc_2003 = l7toa2003_satvi.expression(
  '((satvi - (-0.02318617898610694)) / (0.612232341133361 - (-0.02318617898610694))) * 100',
{
    'satvi': l7toa2003_satvi.select('satvi')
    }).rename('tvfc');

var tvfc_2004 = l7toa2004_satvi.expression(
  '((satvi - (-0.02318617898610694)) / (0.612232341133361 - (-0.02318617898610694))) * 100',
{
    'satvi': l7toa2004_satvi.select('satvi')
    }).rename('tvfc');

var tvfc_2005 = l7toa2005_satvi.expression(
  '((satvi - (-0.02318617898610694)) / (0.612232341133361 - (-0.02318617898610694))) * 100',
{
    'satvi': l7toa2005_satvi.select('satvi')
    }).rename('tvfc');

var tvfc_2006 = l7toa2006_satvi.expression(
  '((satvi - (-0.02318617898610694)) / (0.612232341133361 - (-0.02318617898610694))) * 100',
{
    'satvi': l7toa2006_satvi.select('satvi')
    }).rename('tvfc');

var tvfc_2007 = l7toa2007_satvi.expression(
  '((satvi - (-0.02318617898610694)) / (0.612232341133361 - (-0.02318617898610694))) * 100',
{
    'satvi': l7toa2007_satvi.select('satvi')
    }).rename('tvfc');

var tvfc_2008 = l7toa2008_satvi.expression(
  '((satvi - (-0.02318617898610694)) / (0.612232341133361 - (-0.02318617898610694))) * 100',
{
    'satvi': l7toa2008_satvi.select('satvi')
    }).rename('tvfc');

var tvfc_2009 = l7toa2009_satvi.expression(
  '((satvi - (-0.02318617898610694)) / (0.612232341133361 - (-0.02318617898610694))) * 100',
{
    'satvi': l7toa2009_satvi.select('satvi')
    }).rename('tvfc');
```

```
var tvfc_2010 = l7toa2010_satvi.expression(
  '((satvi - (-0.02318617898610694)) / (0.612232341133361 - (-0.02318617898610694))) * 100',
{
    'satvi': l7toa2010_satvi.select('satvi')
    }).rename('tvfc');

var tvfc_2011 = l7toa2011_satvi.expression(
  '((satvi - (-0.02318617898610694)) / (0.612232341133361 - (-0.02318617898610694))) * 100',
{
    'satvi': l7toa2011_satvi.select('satvi')
    }).rename('tvfc');

var tvfc_2012 = l7toa2012_satvi.expression(
  '((satvi - (-0.02318617898610694)) / (0.612232341133361 - (-0.02318617898610694))) * 100',
{
    'satvi': l7toa2012_satvi.select('satvi')
    }).rename('tvfc');


var tvfc_2013 = l8toa2013_satvi.expression(
  '((satvi - (-0.02318617898610694)) / (0.612232341133361 - (-0.02318617898610694))) * 100',
{
    'satvi': l8toa2013_satvi.select('satvi')
    }).rename('tvfc');
var tvfc_2014 = l8toa2014_satvi.expression(
  '((satvi - (-0.02318617898610694)) / (0.612232341133361 - (-0.02318617898610694))) * 100',
{
    'satvi': l8toa2014_satvi.select('satvi')
    }).rename('tvfc');
var tvfc_2015 = l8toa2015_satvi.expression(
  '((satvi - (-0.02318617898610694)) / (0.612232341133361 - (-0.02318617898610694))) * 100',
{
    'satvi': l8toa2015_satvi.select('satvi')
    }).rename('tvfc');
var tvfc_2016 = l8toa2016_satvi.expression(
  '((satvi - (-0.02318617898610694)) / (0.612232341133361 - (-0.02318617898610694))) * 100',
{
    'satvi': l8toa2016_satvi.select('satvi')
    }).rename('tvfc');
var tvfc_2017 = l8toa2017_satvi.expression(
  '((satvi - (-0.02318617898610694)) / (0.612232341133361 - (-0.02318617898610694))) * 100',
{
    'satvi': l8toa2017_satvi.select('satvi')
    }).rename('tvfc');
var tvfc_2018 = l8toa2018_satvi.expression(
```

```
  '((satvi - (-0.02318617898610694)) / (0.612232341133361 - (-0.02318617898610694))) * 100',
{
    'satvi': l8toa2018_satvi.select('satvi')
    }).rename('tvfc');
var tvfc_2019 = l8toa2019_satvi.expression(
  '((satvi - (-0.02318617898610694)) / (0.612232341133361 - (-0.02318617898610694))) * 100',
{
    'satvi': l8toa2019_satvi.select('satvi')
    }).rename('tvfc');


// Visualise
Map.centerObject(aoi, 10);
Map.addLayer(tvfc_2000.clip(aoi), {min: 0, max: 100, palette: ['red','green','blue']},'tvfc_00',0);
Map.addLayer(tvfc_2005.clip(aoi), {min: 0, max: 100, palette: ['red','green','blue']},'tvfc_05',0);
Map.addLayer(tvfc_2010.clip(aoi), {min: 0, max: 100, palette: ['red','green','blue']},'tvfc_10',0);
Map.addLayer(tvfc_2019.clip(aoi), {min: 0, max: 100, palette: ['red','green','blue']},'tvfc_19',0);

Map.addLayer(tvfc_2000.clip(aoi).addBands(tvfc_2005.clip(aoi)).addBands(tvfc_2010.clip(aoi))
, {min: 0, max: 100}, '2000/2005/2010 RGB', 0);
Map.addLayer(tvfc_2005.clip(aoi).addBands(tvfc_2010.clip(aoi)).addBands(tvfc_2019.clip(aoi))
, {min: 0, max: 100}, '2005/2010/2019 RGB', 0);

////////////////////////////////////////////////////////////////////////////////
//
// Computing the differsnce
//
var diff0005 = tvfc_2005.subtract(tvfc_2000);
var diff0510 = tvfc_2010.subtract(tvfc_2005);
var diff1019 = tvfc_2019.subtract(tvfc_2010);
// Display the differsnce
Map.addLayer(diff0005.clip(aoi), {min: -100, max: 100,palette:
['#d01c8b','#f7f7f7','#4dac26']},'tvfc_0005_diff',0);
Map.addLayer(diff0510.clip(aoi), {min: -100, max: 100,palette:
['#d01c8b','#f7f7f7','#4dac26']},'tvfc_0510_diff',0);
Map.addLayer(diff1019.clip(aoi), {min: -100, max: 100,palette:
['#d01c8b','#f7f7f7','#4dac26']},'tvfc_1019_diff',0);
//
//Calculate histograms for each image
print(ui.Chart.image.histogram({image:diff0005, region:aoi, scale:300}));
print(ui.Chart.image.histogram({image:diff0510, region:aoi, scale:300}));
print(ui.Chart.image.histogram({image:diff1019, region:aoi, scale:300}));
//
// Combine the mean and standard deviation reducers.
var reducers = ee.Reducer.mean().combine({ reducer2: ee.Reducer.stdDev(), sharedInputs: true
});
```

```
//
//Calculate the mean and standard deviation for each difference image
var stats0005 = diff0005.reduceRegion({ reducer: reducers, geometry: aoi, scale: 10, });
var stats0510 = diff0510.reduceRegion({ reducer: reducers, geometry: aoi, scale: 10, });
var stats1019 = diff1019.reduceRegion({ reducer: reducers, geometry: aoi, scale: 10, });
//
//Print the mean and stdv for each difference image
print('stats:', stats0005, stats0510, stats1019);
//
//Apply Thresholds based on < stdvx2 to create a vegetation regrowth mask
var DIFF_UPPER_THRESHOLD0005 = 9.87;
var DIFF_UPPER_THRESHOLD0510 = 8.60;
var DIFF_UPPER_THRESHOLD1019 = 6.98;
var diff0005_thresholded = diff0005.gt(DIFF_UPPER_THRESHOLD0005);
var diff0510_thresholded = diff0510.gt(DIFF_UPPER_THRESHOLD0510);
var diff1019_thresholded = diff1019.gt(DIFF_UPPER_THRESHOLD1019);
//
//Display Masks
Map.addLayer(diff0005_thresholded.updateMask(diff0005_thresholded).clip(aoi),{palette:"gree
n"},'Vegetation gain 00/05',1);
Map.addLayer(diff0510_thresholded.updateMask(diff0510_thresholded).clip(aoi),{palette:"gree
n"},'Vegetation gain 05/10',1);
Map.addLayer(diff1019_thresholded.updateMask(diff1019_thresholded).clip(aoi),{palette:"gree
n"},'Vegetation gain 10/19',1);
//
//Compare differences in vegetation loss between 16/18 and 18/19
var area_gain0005 = diff0005_thresholded.reduceRegion({ reducer: ee.Reducer.sum(),
geometry: aoi, scale: 10, });
var area_gain0510 = diff0510_thresholded.reduceRegion({ reducer: ee.Reducer.sum(),
geometry: aoi, scale: 10, });
var area_gain1019 = diff1019_thresholded.reduceRegion({ reducer: ee.Reducer.sum(),
geometry: aoi, scale: 10, });

//Print the mean and stdv for each difference image
print('stats:',area_gain0005, area_gain0510, area_gain1019);

// Export the tvfc images.
Export.image.toDrive({
image: tvfc_2000.clip(aoi),
description: 'tvfc_2000_2',
scale: 100,
fileFormat: 'GeoTIFF',
});

Export.image.toDrive({
image: tvfc_2005.clip(aoi),
```

```
description: 'tvfc_2005',
scale: 100,
fileFormat: 'GeoTIFF',
});

Export.image.toDrive({
image: tvfc_2010.clip(aoi),
description: 'tvfc_2010',
scale: 100,
fileFormat: 'GeoTIFF',
});

Export.image.toDrive({
image: tvfc_2019.clip(aoi),
description: 'tvfc_2019',
scale: 100,
fileFormat: 'GeoTIFF',
});

// Export the tvfc difference images.
Export.image.toDrive({
image: diff0005.clip(aoi),
description: 'diff0005',
scale: 100,
fileFormat: 'GeoTIFF',
});

Export.image.toDrive({
image: diff0510.clip(aoi),
description: 'diff0510',
scale: 100,
fileFormat: 'GeoTIFF',
});

Export.image.toDrive({
image: diff1019.clip(aoi),
description: 'diff1019',
scale: 100,
fileFormat: 'GeoTIFF',
});

// Export the tvfc significant gain images.
Export.image.toDrive({
image: diff0005_thresholded.clip(aoi),
description: 'diff0005_thresholded',
scale: 100,
```

```
fileFormat: 'GeoTIFF',
});

Export.image.toDrive({
image: diff0510_thresholded.clip(aoi),
description: 'diff0510_thresholded',
scale: 100,
fileFormat: 'GeoTIFF',
});

Export.image.toDrive({
image: diff1019_thresholded.clip(aoi),
description: 'diff1019_thresholded',
scale: 100,
fileFormat: 'GeoTIFF',
});
```

REFERENCES

Angassa, A. (2014). EFFECTS OF GRAZING INTENSITY AND BUSH ENCROACHMENT ON HERBACEOUS SPECIES AND RANGELAND CONDITION IN SOUTHERN ETHIOPIA. *Land Degradation & Development*, *25*(5), 438–451. https://doi.org/10.1002/ldr.2160

Asare, Y. M., Forkuo, E. K., Forkuor, G., & Thiel, M. (2020). Evaluation of gap-filling methods for Landsat 7 ETM+ SLC-off image for LULC classification in a heterogeneous landscape of West Africa. *International Journal of Remote Sensing*, *41*(7), 2544–2564. https://doi.org/10.1080/01431161.2019.1693076

Bekure, S., de Leeuw, P. N., Grandin, B. E., & Neate, P. J. H. (1991). *Maasai herding : an analysis of the livestock production system of Maasai pastoralists in eastern Kajiado District, Kenya*. (S. Bekure, Ed.), *ILCA Systems Study (ILCA). no. 4*. Retrieved from https://books.google.co.ke/books?hl=en&lr=&id=3ioJTPYYdGYC&oi=fnd&pg=PP11&dq=grazing+system+in+kenya&ots=LQ3Hfa6yky&sig=SwyUrKZQoJKvAaCOa_6U7eRoMHE&redir_esc=y#v=onepage&q=grazing system in kenya&f=false

Goldblatt, R., You, W., Hanson, G., Khandelwal, A., Goldblatt, R., You, W., … Khandelwal, A. K. (2016). Detecting the Boundaries of Urban Areas in India: A Dataset for Pixel-Based Image Classification in Google Earth Engine. *Remote Sensing*, *8*(8), 634. https://doi.org/10.3390/rs8080634

Gorelick, N., Hancher, M., Dixon, M., Ilyushchenko, S., Thau, D., & Moore, R. (2017). Google Earth Engine: Planetary-scale geospatial analysis for everyone. *Remote Sensing of Environment*, *202*, 18–27. https://doi.org/10.1016/J.RSE.2017.06.031

Hansen, M. C., Potapov, P. V., Moore, R., Hancher, M., Turubanova, S. A., Tyukavina, A., … Townshend, J. R. G. (2013). High-Resolution Global Maps of 21st-Century Forest Cover Change. *Science*, *342*, 850. https://doi.org/10.1126/science.1244693

Huang, H., Chen, Y., Clinton, N., Wang, J., Wang, X., Liu, C., … Zhu, Z. (2017). Mapping major land cover dynamics in Beijing using all Landsat images in Google Earth Engine. *Remote Sensing of Environment*, *202*, 166–176. https://doi.org/10.1016/J.RSE.2017.02.021

Humanitarian Policy Group. (2010). *Pastoralism demographics, settlement and service provision in the Horn and East Africa Transformation and opportunities: REGLAP (The Regional Livelihoods Advocacy Project)*. Retrieved from www.odi.org.uk/hpg

ICPALD. (2013). *The Contribution of Livestock to the Kenyan Economy POLICY BRIEF SERIES IGAD Center for Pastoral Areas and Livestock Development (ICPALD) The estimation of agricultural GDP in Kenya*. Retrieved from https://igad.int/attachments/714_The Contribution of Livestock to the Kenyan Economy.pdf

KIOKO, J., KIRINGE, J. W., SENO, S. O., KIOKO, J., KIRINGE, J. W., & SENO, S. O. (2012). Impacts of livestock grazing on a savanna grassland in Kenya. *Journal of Arid Land*, *4*(1), 29–35. https://doi.org/10.3724/SP.J.1227.2012.00029

Krätli, S., & Swift, J. (2014). *"Counting Pastoralists" in Kenya*. Retrieved from file:///C:/Users/S.Oloo/Downloads/KratliSwift2014-CountingPastoralistsinKenya.pdf

Lambin, E. F. (2001). Abrupt and periodic shifts in a marsh location and their impact on biodiversity and farming activities in Shompole, Kenya. *International Journal of Remote Sensing*, *22*(5), 711–716. https://doi.org/10.1080/01431160051060084

Ma, Y., Wu, H., Wang, L., Huang, B., Ranjan, R., Zomaya, A., & Jie, W. (2015). Remote sensing big data computing: Challenges and opportunities. *Future Generation Computer Systems*, *51*, 47–60. https://doi.org/10.1016/j.future.2014.10.029

Measham, T. G., & Lumbasi, J. A. (2013). Success factors for community-based natural resource management (CBNRM): Lessons from Kenya and Australia. *Environmental Management*, *52*(3), 649–659. https://doi.org/10.1007/s00267-013-0114-9

Mganga, K. Z., Musimba, N. K. R., & Nyariki, D. M. (2015). Combining Sustainable Land Management Technologies to Combat Land Degradation and Improve Rural Livelihoods in Semi-arid Lands in Kenya. *Environmental Management*, *56*(6), 1538–1548. https://doi.org/10.1007/s00267-015-0579-9

Mureithi, S. M., & Opiyo, F. (2010). Resource use planning under climate change: Experience from Turkana and Pokot pastoralists of Northwestern Kenya. In *2nd International Conference: Climate, Sustainability and Development in Semi-arid Regions*. Retrieved from http://erepository.uonbi.ac.ke/bitstream/handle/11295/81588/Mureithi_Resource use planning under climate change.pdf?sequence=1

Muriithi, F. K. (2016). Land use and land cover (LULC) changes in semi-arid sub-watersheds of Laikipia and Athi River basins, Kenya, as influenced by expanding intensive commercial horticulture. *Remote Sensing Applications: Society and Environment*, *3*, 73–88. https://doi.org/10.1016/j.rsase.2016.01.002

Ng'ethe, J. C. (1992). Group ranch concept and practice in Kenya with special emphasis on Kajiado District. *Future of Livestock Industries in East and Southern Africa: Proceedings of the Workshop Held at Kadoma Ranch Hotel.*, 227. https://doi.org/10.1016/S0955-2863(99)00071-6

Nyland, K. E., Gunn, G. E., Shiklomanov, N. I., Engstrom, R. N., & Streletskiy, D. A. (2018). Land cover change in the lower Yenisei River using dense stacking of landsat imagery in Google Earth Engine. *Remote Sensing*, *10*(8). https://doi.org/10.3390/rs10081226

Ouma, E. A., Obare, G. A., & Staal, S. J. (2003). CATTLE AS ASSETS: ASSESSMENT OF NON-MARKET BENEFITS FROM CATTLE IN SMALLHOLDER KENYAN CROP-LIVESTOCK SYSTEMS. In *Proceedings of the 25th International Conference of Agricultural Economists (IAAE)* (pp. 328–334). Durban, South Africa: Document Transformation Technologies. Retrieved from https://s3.amazonaws.com/academia.edu.documents/36242122/cp03ou04.pdf?AWSAccessKeyId=AKIAIWOWYYGZ2Y53UL3A&Expires=1548298786&Signature=pkLfkykBQP4zpkEfQdQOR5xqsgo%3D&response-content-disposition=inline%3Bfilename%3DCATTLE_AS_ASSETS_ASSESSMENT_OF_NON-MA

Padarian, J., Minasny, B., & McBratney, A. B. (2015). Using Google's cloud-based platform for digital soil mapping. *Computers & Geosciences*, *83*, 80–88. https://doi.org/10.1016/J.CAGEO.2015.06.023

Patel, N. N., Angiuli, E., Gamba, P., Gaughan, A., Lisini, G., Stevens, F. R., … Trianni, G. (2015). Multitemporal settlement and population mapping from Landsat using Google Earth Engine. *International Journal of Applied Earth Observation and Geoinformation*, *35*, 199–208. https://doi.org/10.1016/J.JAG.2014.09.005

Reeves, M. C., Tennessee, R. A., Hunt, E. R. J., Wasantha, R., Lalit, K., Loboda, T., … Ramsey, R. D. (2016). Global View of Remote Sensing of Rangelands: Evolution, Applications, Future Pathways. *Land Rresources Monitoring, Modeling, and Mapping with Remote Sensing*, 237–275. Retrieved from https://www.fs.fed.us/rm/pubs_journals/2015/rmrs_2015_reeves_m001.pdf

SORALO | South Rift Association of Land Owners. (n.d.). Retrieved June 20, 2020, from http://www.soralo.org/

SRM. (2019). Society of Range Management Glossary | Global Rangelands. Retrieved January

27, 2019, from https://globalrangelands.org/glossary/R?term=

Tueller, P. T. (1989). Remote sensing applications technology for rangeland management. *Journal of Range Management*, *42*(6), 442–453. Retrieved from https://journals.uair.arizona.edu/index.php/jrm/article/viewFile/8418/8030

Waithaka, J. (2004). Maasai Mara - An ecosystem under siege: An African case study on the societal dimension of rangeland conservation. In *African Journal of Range and Forage Science* (Vol. 21, pp. 79–88). Taylor & Francis Group. https://doi.org/10.2989/10220110409485838

Williams, D. L., Goward, S., & Arvidson, T. (2006). Landsat: Yesterday, today, and tomorrow. *Photogrammetric Engineering and Remote Sensing*. American Society for Photogrammetry and Remote Sensing. https://doi.org/10.14358/PERS.72.10.1171